# Analytical Methods

Accepted Manuscript

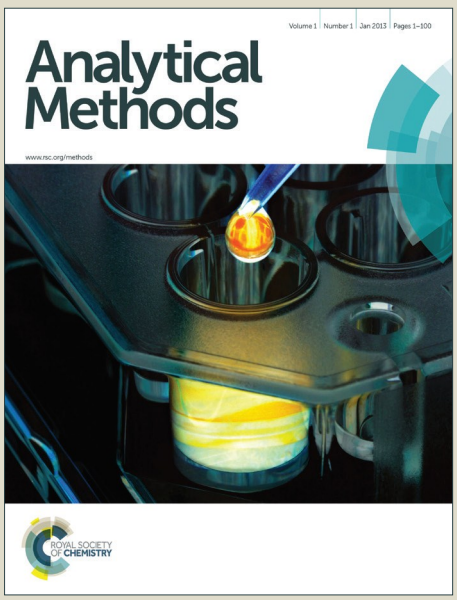


This is an *Accepted Manuscript*, which has been through the Royal Society of Chemistry peer review process and has been accepted for publication.

*Accepted Manuscripts* are published online shortly after acceptance, before technical editing, formatting and proof reading. Using this free service, authors can make their results available to the community, in citable form, before we publish the edited article. We will replace this *Accepted Manuscript* with the edited and formatted *Advance Article* as soon as it is available.

You can find more information about *Accepted Manuscripts* in the Information for Authors.

Please note that technical editing may introduce minor changes to the text and/or graphics, which may alter content. The journal's standard Terms & Conditions and the Ethical guidelines still apply. In no event shall the Royal Society of Chemistry be held responsible for any errors or omissions in this *Accepted Manuscript* or any consequences arising from the use of any information it contains.

ROYAL SOCIETY OF CHEMISTRY

www.rsc.org/methods

Journal Name

ARTICLE

# Evaluation of antioxidant activity of phenols and tannic acid determination with $Mn_3O_4$ nano-octahedrons as oxidase mimic

Received 00th January 20xx,
Accepted 00th January 20xx

DOI: 10.1039/x0xx00000x

www.rsc.org/

Xiaodan Zhang, Yuming Huang*

In the paper, we successfully synthesized novel $Mn_3O_4$ nano-octahedrons by a simple hydrothermal method and demonstrated that the prepared $Mn_3O_4$ nanoparticles (NPs) exhibited highly intrinsic oxidase-like activity and could catalyze the reaction of TMB, ABTS and OPD to produce a typical color reaction in the absence of $H_2O_2$ within minutes. Compared with other non-noble metal NPs oxidase nanozymes, the affinity of $Mn_3O_4$ NPs to TMB was increased by at least 35% according to the $K_m$ values. It was deduced that $O_2^{\bullet-}$ and few OH· radicals were produced during the catalytical reaction. Then, the addition of twelve phenols to the TMB-$Mn_3O_4$ NPs system led to the fading of the solution by different degrees based on the antioxidant activity of phenols. Thus, preliminary assessment of the antioxidant ability of twelve phenols by TMB decolorization assay was realized based on the excellent oxidase-like properties of the $Mn_3O_4$ NPs. Finally, under the optimum conditions, visual determination of tannic acid (TA) was realized and the detection limit was 19 nM with a linear range from 0.05 to 1.4 μM. The propsed method was succesfully used to detemine TA in tea samples.

## 1. Introduction

Inorganic nanomaterials possessed the enzyme-like activities were called nanozymes, such as peroxidase-like activity, oxidase-like and SOD/catalase-like activity of nanomaterials. In contrast with natural enzymes, nanozymes own the remarkable merits, such as easy to preparation, low-cost, controllable in catalytic activity and stable against harsh conditions, thus possessing a promising future in enzyme-related applications. Since ferromagnetic nanoparticles (NPs) was exciting discovered as peroxidase mimetic for the first time[1], large amount of nanozymes were emerged in the following years, and they have been used as effective colorimetric tools for biosensing[2], immunoassay[3], environmental monitoring[4] and so on. Until now, they are still a hot research area. However, the majority of these analysis methods are based on the peroxidase mimetic property of nanomaterials, which could catalyze the oxidation of the typical chromogenic substrates using $H_2O_2$ as an oxidant, while the addition of high concentration of $H_2O_2$ would make the application difficult because of the unstable and destructive of $H_2O_2$. Thus, it was necessary to develop novel enzyme mimetics for better applications.

Oxidase enzymes that can catalyze the oxidation of substrates simply employing molecular oxygen as the electron acceptor are more facile, economic and environmental. Actually, some peroxidase nanozymes also exhibited the oxidase-like property such as $CeO_2$ NPs[5], Au@Pt nanostructures[6], $MnO_2$ nanomaterials[7], Fe-Co NPs[8], $CoFe_2O_4$ NPs[9] and polyoxometalate (POMs) NPs[10]. Nevertheless, almost all of the analytical applications of these nanozymes were only focused on their peroxidase-like catalytic activities, while their oxidase-like enzyme character was often overlooked. Only a few attempts have been made to investigate the analytical applications based on the oxidase mimetic activities of nanomaterials. For example, investigators have found that naked 3.6 nm Au NPs exhibited glucose oxidase-like activity, was capable of catalyzing the aerobic oxidation of glucose to gluconate under mild conditions[11]. The oxidase mimic of Au@Pt nanorods has been used as a screening tool for enzyme inhibitors, and selective and quantitative detection of $Hg^{2+}$ ions was realized[12]. Recently, Hu *et al*. have fabricated three-dimensional (3D) nano-assemblies of noble metal Au/Ag NPs as an oxidase mimic for catalyzing the degradation of methyl blue (MB)[13]. However, all of these analytical application based on the oxidase mimics were prepared by noble metals with a complicated preparation method which are not economically and time-consuming. So it is necessary to develop oxidase mimics of non-noble metal nanomaterials and the related work is scarce. For instance, polymer-coated $CeO_2$ NPs, $MnO_2$ nanowires and folate-functionalized POMs have been employed as an oxidase-like biocatalyst for immunosorbent assay[14] and an increasing concern on POMs is emerged because of the excellent catalytic properties of POMs[15]; Metal oxide NPs of $CoFe_2O_4$ were found to possess oxidase-like activity in our early investigation and were used to determine sulfite based on luminol chemiluminescence[16].

In recent years, manganese oxides are of extensively interest in many applications due to their outstanding structural flexibility combined with novel physical and chemical properties. Among the studied manganese oxides, $Mn_3O_4$ posses many excellent

*Key Laboratory of Luminescent and Real-time Analytical Chemistry, Ministry of Education, College of Chemistry and Chemical Engineering, Southwest University, Chongqing 400715, P. R. China. E-mail: ymhuang@swu.edu.cn*

† Electronic Supplementary Information (ESI) available: Supporting figures and tables. See DOI: 10.1039/x0xx00000x

properties due to its unique mixed-valance sate, high activity, durability, and low cost. For example, as an effective catalyst for oxidation and reduction reactions, $Mn_3O_4$ has played the role of catalyst for the oxidation of methane[17], phenolic contaminants[18] and the degradation of dyes[19], or the reduction of nitrobenzene[20]. But to our knowledge, the investigation of the enzyme-like activity of $Mn_3O_4$ NPs has not been reported.

In this study, we investigated the potential enzyme mimic activity of $Mn_3O_4$ NPs. As expected, it was found that $Mn_3O_4$ NPs could effectively catalyze the reaction of organic substrates [3,3,5,5-tetramethylbenzidine (TMB), *o*-phenylenediamine (OPD) and (2,2'-azino-bis(3-ethylbenzothiazoline-6-sulfonic acid) diammonium salt (ABTS)] to produce the typical colors in the absence of $H_2O_2$. Then, we utilized the noncarcinogenic TMB system as a model enzyme-like reaction to investigate the oxidase-like catalytic property of $Mn_3O_4$ NPs. Furthermore, we preliminary evaluated the antioxidant ability of twelve phenols based on the possible mechanism that the production of radicals during the TMB colorimetric reaction. Finally, the antioxidant tendency of phenols in the results with the TMB-$Mn_3O_4$ NPs system was similar trends with Folin-Ciocalteu (F-C) method, which was regarded as a measurement of overall antioxidant capacity rather than phenolic content suggested by investigators[21]. Thus, we proposed a method for preliminary assessing the antioxidant ability of twelve phenols by TMB decolorization assay. As an analytical method, finally, tannic acid (TA) was used as an example to prove the real application of TMB-$Mn_3O_4$ NPs system with satisfactory results.

## 2. Experimental

### 2.1 Reagents

All the reagents used in the experiments were analytical grade and used without further purification. Potassium permanganate ($KMnO_4$) was purchased from Tianjin Guangfu Fine Chemical Research Institute (Tianjin, China), and TMB was purchased from Sigma-Aldrich and stored in a refrigerator at 4 °C. Disodium ethylene diaminetetra-acetate dihydrate (EDTA-2Na·2$H_2O$), tannic acid, gallic acid, pyrogallol, catechol, *m*-dihydroxybenzene, hydroquinone, phloroglucin, 2,4-dichlorophenol, pentachlorophenol, *p*-nitrophenol, 2,4,6-trinitrophenol, and phenol were all of analytical grade and purchased from Chongqing Chemical Reagents Company (Chongqing, China). The working solutions were prepared fresh daily and diluted by ultra-pure water for further use. Ultra-pure water was used in all experiments. All glassware was soaked in 10% nitric acid and thoroughly cleaned before use.

### 2.2 Preparation of $Mn_3O_4$ NPs

The $Mn_3O_4$ NPs were prepared by the hydrothermal synthesis method[22]. Simply, 4 mL 0.5 M EDTA-2Na aqueous solution was firstly added into 10 mL 0.2 M $KMnO_4$ aqueous solution under stirring, and the color of solution changed from purple to black-brown immediately when they were mixed together which referred to the formation of a stable complex. Secondly, the mixed solution was transferred into a 100 mL Teflon cup, and then filled with ultra-pure water up to about 70 mL. Then, 2 M $HNO_3$ was used to adjust the pH of the solution to 6.0 under vigorous magnetic stirring for 10 min. The Teflon-lined stainless steel autoclave was sealed and maintained in the oven at 180 °C for 4 h and was cooled down to room temperature. The light brown products was obtained by filtration, washed with ultra-pure water for several times and followed with ethanol, then dried at 60 °C for 6 h. In the following experiments, the nanoparticles were ultrasonic dispersed in ultra-pure water directly to a certain concentration before use.

### 2.3 Instrumentations

Absorption measurements were performed on a UV-2450 spectrophotometer (Shimadzu, Japan). The pH of the solution was detected by a PHS-3D precision pH meter (Shanghai Precision Scientific Instruments Co., Ltd., China). The transmission electron microscopy (TEM) images of $Mn_3O_4$ NPs were obtained from Tecnai G2 20 (FEI, USA) operating at 200 kV, and equipped with an energy dispersive X-ray spectrometer (EDX) for elemental analysis. The scanning electron microscopy (SEM) images were obtained from an S-4800 field emission scanning electron microscope (Hitachi, Japan) with an accelerating voltage of 15 kV. The X-ray diffraction (XRD) pattern of the as-prepared products was measured using an XD-3 X-ray diffractometer (PuXi, Beijing, China) under the condition of nickel filtered Cu-Kα radiation (λ=0.15406 nm) at current of 20 mA and a voltage of 36 kV. The scanning rate was 4° $min^{-1}$ in the angular range of 10–70° (2$\theta$). The Fourier transform infrared (FT-IR) spectrum of the as prepared $Mn_3O_4$ was obtained using a Tenson 27 Fourier Transform Infrared spectrometer (Bruker, Germany).

### 2.4 General procedure for colorimetric detection and antioxidant activity assessment of phenols

In a typical process, the aqueous solution of $Mn_3O_4$ NPs with concentration of 5 mg/L was added to TMB solution (final concentration of $10^{-4}$ M) in the presence of acetate buffer (pH 3.5). The mixture was incubated at 35 °C for 30 min. Then the UV-vis spectra measurements and photographs were taken. In order to evaluate the effects of various factors on the oxidase-like activity of the $Mn_3O_4$ NPs, the relative activity was used as criterion. The maximum point in each curve was set as 100%. Hence, the relative activity was defined as the ratio of absorbance at target point to the maximum point.

For assessing the antioxidant activity of different phenols by the proposed method, 0.25 mL each of phenols of $10^{-4}$ M was mixed with 0.5 mL of $10^{-3}$ M TMB, 0.25 mL of 100 mg/L $Mn_3O_4$ NPs, and 4 mL of 0.2 M NaAc buffer (pH 3.5) for 30 min of incubation at 35 °C. Then the maximum absorbance at 655 nm was recorded. This TMB method to measure the relative antioxidant activity of phenols was expressed as the inhibitory ratio of the TMB-$Mn_3O_4$ colorimetric reaction after the addition of phenols to the system. Relative absorbance of $(A^0_{655nm}-A_{655nm})/A^0_{655nm}$ was used.

The F-C method described by the International Organization for Standardization (ISO) 14502-1 was used[23]. Briefly, 5.0 mL of 10% (v/v) Folin-Ciocalteu's reagent was firstly mixed with 1.0 mL of diluted phenol working solution for 5 min. Then 4.0 mL of 7.5% (w/v) sodium carbonate solution was added and well mixed. The mixture was allowed to stand at room temperature for 60 min and then measured the maximum absorbance at 765 nm ($A_{765nm}$). The relative antioxidant activity of the phenols was expressed as the relative activity. In the colorimetric reaction of different phenols

with F-C reagent, the $A_{765nm}$ values were recorded, among which the maximum value was set as 100% and the relative activity was defined as the ratio of absorbance at target value to the maximum value.

#### 2.6 Procedures for determination of tannic acid in tea samples

For TA determination in tea, three tea samples taken from the local supermarket were chosen. 0.2 g of tea sample was added to 50 mL of ultra-pure water, and the mixture was boiled for 10 min, naturally cooled to room temperature, then filtrated through 0.22 $\mu$m micropore membrane and the filtrate was collected[24] and diluted to 50 mL with ultra-pure water. This solution was further diluted for analysis. Then, under the optimum conditions, 0.5 mL of the diluted filtrate was mixed with 0.5 mL of $10^{-3}$ M TMB, 0.25 mL of 10 mg/L $Mn_3O_4$ NPs, and 3.75 mL of 0.2 M acetate buffer (pH 4.0). And then the mixture was incubated at 35 °C for 30 min. Finally, the UV-vis absorbance at 655 nm was detected. The reduction values of the absorbance at 655 nm ($\Delta A=A_0-A_i$) ($A_0$ and $A_i$ were the absorbance without TA and that with a TA concentration of i, respectively) *versus* the different concentrations of TA were used for the calibration curve for TA. The content of TA in the samples was quantified by the standard curve method.

## 3. Results and Discussion

#### 3.1 Characterization of $Mn_3O_4$ NPs

The SEM image (Fig. 1A) showed the morphology of the $Mn_3O_4$ NPs was almost octahedron. Though the size distribution of $Mn_3O_4$ nano-octahedrons was not uniform, the facets of octahedrons were smooth and the size length of square base of octahedrons of larger nano-octahedrons was about 150 nm. The TEM image of the individual nano-octahedron in the Fig. S1 (see ESI†) also proved the uniform tetragonal shape of the $Mn_3O_4$ NPs which was consistent with the SEM analysis. The analysis of EDX (Fig. S1, ESI†) confirmed that the finely crystallized nano-octahedrons were composed of Mn and O without other impurities.

The XRD pattern of the as-synthesized sample was shown in Fig. 1B. As the reported results in the literature[22, 25], the as-obtained product was well crystallized and all diffraction peaks were well assigned to the tetragonal structure of hausmannite $Mn_3O_4$ except to a very small fraction peaks of pyrolusite $MnO_2$ marked with asterisks.

The FT-IR absorption spectrum of the $Mn_3O_4$ NPs was shown in Fig. S2 (see ESI†). Three significant absorption bands were displayed in the range of 400-650 $cm^{-1}$. The vibration frequency located at 628 $cm^{-1}$ and 520 $cm^{-1}$ were characteristic of Mn-O stretching modes in tetrahedral sites and octahedral sites, respectively, and the vibration band located at 410 $cm^{-1}$ could be assigned to the vibration of manganese species ($Mn^{3+}$-O) in the octahedral site of $Mn_3O_4$[26]. Moreover, the broad absorption band at 3420 and 3163 $cm^{-1}$ could be attributed to the O-H stretching vibrating mode of the absorbed water, and the bands at 1638, 1401, 1108 $cm^{-1}$ should be attributed to the Mn-OH vibration[27]. All the characteristic results above indicated that the prepared material was $Mn_3O_4$.

#### 3.2 Characterization of oxidase-like activity of $Mn_3O_4$ NPs

The enzyme-like activity of $Mn_3O_4$ NPs was investigated by using TMB as the enzyme substrate. As was expected, the as prepared $Mn_3O_4$ NPs could catalyze the oxidation of TMB quickly even in the absence of $H_2O_2$ to produce a typical blue colour. And the oxidative product of TMB showed a maximum absorbance peak at 655 nm as shown in Fig. 2A, which indicated the efficient catalysis of $Mn_3O_4$ NPs and it could be act as oxidase mimic. Also the $Mn_3O_4$ NPs could catalyze the oxidation reaction of other enzyme substrates without $H_2O_2$, such as ABTS and OPD, to produce their typical colors, respectively, as shown in Fig. 2A. From the curve of time-dependent absorbance changes at 655 nm of TMB in Fig. 2B, it was found that the rate of $Mn_3O_4$ NPs-catalyzed reaction of the oxidation of TMB was raised steeply within 5 min and then kept steady. The absorbance slope of TMB-$Mn_3O_4$ NPs system at 655 nm was much higher than the autoxidation of TMB. These results proved the excellent oxidase-like activity of $Mn_3O_4$ NPs. After the solution was purged with nitrogen, the catalytic reaction rate of TMB oxidation decreased quickly as shown in Fig. 2B, which indicated that the dissolved oxygen involved in the TMB oxidation. So we presumed that the oxidase mimic activity of $Mn_3O_4$ NPs derived from the catalytic reduction of dissolved oxygen with $Mn_3O_4$ NPs.

#### 3.3 Possible reaction mechanism

To prove the possible reaction mechanism, it is essential to illustrate the produce of reactive oxygen species (ROS) from the decomposition of molecular oxygen catalyzed by $Mn_3O_4$ NPs. Manganese oxides were known to be active catalysts and they also have been applied as oxygen storage components. It has been proved that the oxygen absorption behavior of manganese oxide was superior to that of cerium oxide[28]. $Mn_3O_4$ NPs included the valence of $Mn^{2+}/Mn^{3+}$, and manganese transfer electrons to $O_2$ causes the formation of superoxide anions ($O_2^{\bullet-}$)[29] as the following reaction (eq. (1)). $O_2^{\bullet-}$ would be expected to produce $H_2O_2$ partly by nonenzymatic or SOD-catalyzed dismutation[30] (eq. (2)). Furthermore, it was possible that the small quantity of $H_2O_2$ was decomposed into hydroxyl radicals (OH·) in the presence of transition metal ions[30] (eq. (3)). Then, $O_2^{\bullet-}$/OH· and $Mn^{3+}$ might further oxidize the enzyme substrate to give the relative color. So, we presume that $O_2^{\bullet-}$ and few OH· radicals may produce in this TMB-$Mn_3O_4$ NPs-$O_2$ system.

$$Mn^{2+} + O_2 \longrightarrow Mn^{3+} + O_2^{\bullet-} \quad (1)$$

$$O_2^{\bullet-} + H^+ \longrightarrow H_2O_2 + O_2 \quad (2)$$

$$Mn^{2+} + H_2O_2 \longrightarrow Mn^{3+} + OH^- + OH\cdot \quad (3)$$

In order to validate above presumption, we added radical inhibitors into the system. It was known that *t*-butyl alcohol was a strong OH· radical scavenger[31] and *p*-benzoquinone was able to trap superoxide anions radicals effectively[32]. As shown in Fig. S3 (see ESI†), the addition of 1 mM *p*-benzoquinone inhibited the color reaction obviously, when 20 mM *t*-butyl alcohol only had little effect. So from the results we could deduced that $O_2^{\bullet-}$ radicals were generated mainly during this catalytic reaction as well as few OH· radicals. The results were well matched with our deduced above, that is, the oxygen free radicals ($O_2^{\bullet-}$/OH·) were originated from the reduction of dissolved oxygen adsorbed on the $Mn_3O_4$ NPs

surface, which further confirmed that the dissolved oxygen participated in the TMB-$Mn_3O_4$ NPs system. Based on above discussion, the possible reaction mechanism of the TMB-$Mn_3O_4$ NPs system was summarized in Scheme 1.

### 3.4 Oxidase-like activity of pH, temperature and $Mn_3O_4$ NPs dependence

In order to ensure the reaction proceeding completely, 30 min was chose for incubation in the following experiments. The catalytic activity of the $Mn_3O_4$ NPs was similar to the nature enzyme, depending on pH, temperature and the concentration of catalyst. We varied the pH from 1.0 to 12.0, the temperature from 25 to 65 °C, and the concentration of the $Mn_3O_4$ NPs from 1.0 to 9.0 mg/L to measure the oxidase-like activity of the $Mn_3O_4$ NPs. Results in Fig. S4 (see ESI†) indicated that the optimal pH and temperature for the $Mn_3O_4$ NPs were 3.5 and 35 °C, respectively. Similar to HRP, the catalytic activity of $Mn_3O_4$ NPs in acidic medium was much higher than that in neutral or basic solutions, resulting from the acid-promoted colorimetric reaction of TMB[33]. So the nature of pH dependent catalytic activity was primarily referred to the substrate TMB itself rather than the nano-catalyst. The absorbance at 655 nm was increasing with the increase of the concentration of $Mn_3O_4$ NPs in the system, considering saving the reagent, we finally chose 5 mg/L as the optimal concentration of $Mn_3O_4$ NPs.

### 3.5 Stability of $Mn_3O_4$ NPs and kinetic analysis

As an inorganic nanomaterial, $Mn_3O_4$ NPs was considered to be more stable than the natural enzyme, and the stability of the $Mn_3O_4$ NPs in a wide range of pH and temperature was investigated. After incubating the $Mn_3O_4$ NPs at a range of pH and temperature for 2 h, respectively, we measured its catalytic activity under the standard conditions. It was found that the relative activity of $Mn_3O_4$ NPs still remained above 80% over the wide range of pH 1 to 12 and temperature 20 to 80 °C (Fig. S5, ESI†). So the application of $Mn_3O_4$ NPs was feasible under harsh conditions due to its robustness. Besides, the catalytic activity study suggested that the batch-to-batch reproducibility among three $Mn_3O_4$ NPs prepared at different times is satisfactory with relative standard deviation (RSD) less than 5% (Table S1, ESI†). After one month storage, the relative catalytic activity of the $Mn_3O_4$ NPs was maintained above 88% (Fig. S6, ESI†), showing their long-term storage stability. This is because the zeta potential of the $Mn_3O_4$ suspensions was determined to be about −12.6 mV at pH 3.5, indicating the negatively charged surface of the $Mn_3O_4$ suspensions. Hence, the $Mn_3O_4$ suspensions maintain good stability due to their strong electrostatic repulsion effects.

To determine the steady-state kinetic parameters and obtain the typical Michaelis-Menten curve, double reciprocal plot between the initial reaction velocity ($v$) and the concentration of TMB was presented under the optimal conditions. The Michaelis–Menten constant ($K_m$) and maximum reaction ($V_{max}$) were calculated from the linear fitting in Fig. 3. It was known that $K_m$ value reflected the affinity to substrate for a natural enzyme, and the lower $K_m$ value, the higher affinity between the substrate and enzyme. For the oxidization of TMB by dissolved oxygen, the $K_m$ value of $Mn_3O_4$ NPs was lower than that of $Fe_3O_4$, $Co_3O_4$ NPs, nanoceria and BSA-$MnO_2$ NPs except noble metal Au@Pt nanorods (Table 1). Compared with the non-noble metal NPs, the affinity of the as-prepared $Mn_3O_4$ NPs to TMB was enhanced by at least 35%, which may be due to the special nano-octahedrons structure. All the data shown that $Mn_3O_4$ NPs was an oxidase mimic with high catalytic activity.

### 3.6 Application of the TMB-$Mn_3O_4$ NPs system for antioxidant activity assessment of phenols and tannic acid detection

Phenolic compounds are usually existed in various plants and foods, and they have been known to have numerous biological effects such as antioxidant activity. Till now, two free radicals were usually used for assessing antioxidant activity, namely, $ABTS^{+\bullet}$ and 2,2-diphenyl-1-picrylhydrazyl ($DPPH^{\bullet}$)[35]. Both methods were based on the free radical scavenging assay, a reaction of an antioxidant with a radical ($ABTS^{+\bullet}$ or $DPPH^{\bullet}$), resulting in the decrease in radical's characteristic absorbance[36]. Similarly, when the phenols were added to the TMB–$Mn_3O_4$ NPs system, the $TMB^{+\bullet}$ radical's characteristic absorbance were decreased. So it was possible to use the TMB decolorization assay to evaluate the antioxidant activity of phenols.

In this research, under the same reaction conditions, we investigated the inhibition effects of twelve phenols on the TMB–$Mn_3O_4$ NPs system to preliminary assess their antioxidant abilities, and the results of inhibiting potency were contrasted with the F-C method. The antioxidant tendency in the results obtained by the proposed method was in agreement with those obtained by the F-C colorimetric method, as shown in Fig. 4. From the results, TA exhibited the most obvious inhibitory effect on the TMB-$Mn_3O_4$ system and the most enhancement effect on F-C reaction, respectively, which indicated the strongest antioxidant capacity of TA with the two different methods. Also, from Fig. 4, we can conclude that the relative antioxidant activity of these phenols greatly increased with the increased number of –OH group in these phenols, and the phenols with relative highly antioxidant activity was in the following decreasing order: tannic acid > gallic acid > pyrogallol, which was also identical with the previous results[37]. Thus, it has the potential to use the TMB-$Mn_3O_4$ NPs system for the preliminary assessment of phenols' antioxidant activity.

The determination of tannic acid was chose as an example to investigate the possibility of TMB-$O_2$-$Mn_3O_4$ NPs system in real samples. Firstly, the optimum reaction conditions in the present of 1 μM TA were studied and the results were obtained as follows: pH 4.0 (0.2 M acetate buffer), 35 °C and 5 mg/L $Mn_3O_4$ NPs (Fig. S7, ESI†). Under the optimum conditions, the visual detection of TA was realized, and the calibration data for 0.05–1.4 μM was well described by the equation: $\Delta A = 0.389 c_{TA} + 0.0189$ ($R^2 = 0.9934$, n=8) (Fig. 5), where $\Delta A$ was the inhibited absorbance intensity when TA was added in the TMB-$O_2$-$Mn_3O_4$ NPs system, and $c$ was TA concentration (μM). The limit of detection (LOD) was 19 nM (3σ). Then, the proposed method was applied to analyze tannic acid in three tea samples. Recovery tests were also carried out on the samples. From the results (Table S2, ESI†), the recoveries for the spiked tea samples ranged from 93.4 to 108.7% at three spiked concentration levels. These results indicated that the proposed method was satisfactory for the real sample analysis.

## Conclusions

In summary, we have successfully synthesized $Mn_3O_4$ NPs with a simple hydrothermal method and demonstrated its intrinsic oxidase-like activity. The $Mn_3O_4$ NPs showed a good affinity to TMB due to the small $K_m$ value of 0.025 mM from the typical Michaelis-Menten curve, and the affinity was increased by 35.9% at least compared with other non-noble metal NPs oxidase nanozymes. We deduced that the oxygen free radicals ($O_2^{\bullet-}$/OH·) were originated from the reduction of dissolved oxygen adsorbed on the $Mn_3O_4$ NPs surface. Based on the inhibition of twelve phenols to the TMB-$Mn_3O_4$ NPs system, we developed a simple method to preliminary screen the antioxidant activity of phenols. On this basis, a simple and sensitive colorimetric assay for tannic acid in tea samples was developed and as low as 19 nM TA could be detected by this method.

## Acknowledgements

The financial support of the research by the Fundamental Research Funds for the Central Universities (XDJK2013C114) and the Natural Science Foundation of China (No. 21075099) are gratefully acknowledged.

## Notes and references


1 L. Z. Gao, J. Zhuang, L. Nie, J. B. Zhang, Y. Zhang, N. Gu, T. H. Wang, J. Feng, D. L. Yang, S. Perrett and X. Yan, *Nat. Nanotechnol.*, 2007, **2**, 577-583.

2 (a) L. Q. Yang, X. L. Ren, F. Q. Tang and L. Zhang, *Biosens. Bioelectron.*, 2009, **25**, 889-895; (b) M. I. Kim, J. Shim, T. Li, M. A. Woo, D. Cho, J. Lee and H. G. Park, *Analyst*, 2012, **137**, 1137-1143; (c) W. Dong, X. Liu, W. Shi and Y. Huang, *RSC Adv.,* 2015, **5**, 17451–17457.

3 (a) L. Z. Gao, J. M. Wu, S. Lyle, K. Zehr, L. L. Cao and D. Gao, *J. Phys. Chem. C*, 2008, **112**, 17357-17361; (b) J. M. Perez, *Nat. Nanotechnol.*, 2007, **2**, 535-536.

4 (a) J. Zhuang, J. B. Zhang, L. Z. Gao, Y. Zhang, N. Gu, J. Feng, D. L. Yang and X. Y. Yan, *Mater. Lett.*, 2008, **62**, 3972-3974; (b) Y. S. Kim and J. Jurng, *Sensor. Actuat. B-Chem.*, 2013, **176**, 253-257; (c) J. B. Zhang, J. Zhuang, L. Z. Gao, Y. Zhang, N. Gu, J. Feng, D. L. Yang, J. D. Zhu and X. Y. Yan, *Chemosphere*, 2008, **73**, 1524-1528.

5 X. Jiao, H. J. Song, H. H. Zhao, W. Bai, L. C. Zhang and Y. Lv, *Anal. Methods*, 2012, **4**, 3261-3267.

6 W. W. He, Y. Liu, J. S. Yuan, J. J. Yin, X. C. Wu, X. N. Hu, K. Zhang, J. B. Liu, C. Y. Chen, Y. L. Ji and Y. T. Guo, *Biomaterials*, 2011, **32**, 1139-1147.

7 X. Liu, Q. Wang, H. H. Zhao, L. C. Zhang, Y. Y. Su and Y. Lv, *Analyst*, 2012, **137**, 4552-4558.

8 Y. Chen, H. Cao, W. Shi, H. Liu and Y. Huang, *Chem. Commun.*, 2013, **49**, 5013-5015.

9 (a) W. Shi, X. Zhang, S. He and Y. Huang, *Chem. Commun.*, 2011, **47**, 10785-10787; (b) Y. Fan, W. Shi, X. Zhang and Y. Huang, *J. Mater. Chem. A,* 2014, **2**, 2482–2486.

10 J. J. Wang, D. X. Han, X. H. Wang, B. Qi and M. S. Zhao, *Biosens. Bioelectron.*, 2012, **36**, 18-21.

11 M. Comotti, C. Della Pina, R. Matarrese and M. Rossi, *Angew. Chem. Int. Ed. Engl.*, 2004, **43**, 5812-5815.

12 J. B. Liu, X. N. Hu, S. Hou, T. Wen, W. Q. Liu, X. Zhu and X. C. Wu, *Chem. Commun.*, 2011, **47**, 10981-10983.

13 L. Wang, Y. Zeng, A. Shen, X. Zhou and J. Hu, *Chem. Commun.*, 2015, **51**, 2052-2055.

14 (a) A. Asati, S. Santra, C. Kaittanis, S. Nath and J. M. Perez, *Angew. Chem. Int. Ed. Engl.*, 2009, **48**, 2308-2312; (b) J. Wang, X. Mi, H. Guan, X. Wang and Y. Wu, *Chem. Commun.*, 2011, **47**, 2940-2942; (c) Y. Wan, P. Qi, D. Zhang, J. J. Wu and Y. Wang, *Biosens. Bioelectron.*, 2012, **33**, 69-74; (d) Y. Ji, J. Xu, X. L. Chen, L. Han, X. H. Wang, F. Chai and M. S. Zhao, *Sensor. Actuat. B-Chem.,* 2015, **208**, 497-504.

15 (a) S. S. Wang and G. Y. Yang, *Chem. Rev.,* 2015, **115**, 4893-4962; (b) X. B. Han, Y. G. Li, Z. M. Zhang, H. Q. Tan, Y. Lu and E. B. Wang, *J. Am. Chem. Soc.,* 2015, **137**, 5486-5493.

16 X. Zhang, S. He, Z. Chen and Y. Huang, *J. Agric. Food Chem.*, 2013, **61**, 840-847.

17 E. R. Stobbe, B. A. de Boer and J. W. Geus, *Catal. Today*, 1999, **47**, 161-167.

18 E. Saputra, S. Muhammad, H. Sun, H. M. Ang, M. O. Tade and S. Wang, *J. Colloid Interface Sci.*, 2013, **407**, 467-473.

19 Z. C. Bai, B. Sun, N. Fan, Z. C. Ju, M. H. Li, L. Q. Xu and Y. T. Qian, *Chem.-Eur. J.*, 2012, **18**, 5319-5324.

20 E. J. Grootendorst, Y. Verbeek and V. Ponec, *J. Catal.*, 1995, **157**, 706-712.

21 J. D. Everette, Q. M. Bryant, A. M. Green, Y. A. Abbey, G. W. Wangila and R. B. Walker, *J. Agric. Food Chem.*, 2010, **58**, 8139-8144.

22 H. Jiang, T. Zhao, C. Y. Yan, J. Ma and C. Z. Li, *Nanoscale*, 2010, **2**, 2195-2198.

23 ISO 14502-1: 2005. Determination of substances characteristic of green and black tea-Part 1: Content of total polyphenols in tea-Colorimetric method using Folin-Ciocalteu reagent.

24 S. L. Feng, A. Tang, J. H. Jiang and J. Fan, *Anal. Chim. Acta*, 2002, **455**, 187-191.

25 Y. Li, H. Y. Tan, X. Y. Yang, B. Goris, J. Verbeeck, S. Bals, P. Colson, R. Cloots, G. Van Tendeloo and B. L. Su, *Small*, 2011, **7**, 475-483.

26 (a) N. Gupta, A. Verma, S. C. Kashyap and D. C. Dube, *J. Magn. Magn. Mater.*, 2007, **308**, 137-142; (b) S. Lanfredi, P. S. Saia, R. Lebullenger and A. C. Hernandes, *Solid State Ionics*, 2002, **146**, 329-339; (c) W. Z. Wang, C. K. Xu, G. H. Wang, Y. K. Liu and C. L. Zheng, *Adv. Mater.*, 2002, **14**, 837-840.

27 A. B. Yuan and Q. L. Zhang, *Electrochem. Commun.*, 2006, **8**, 1173-1178.

28 Y. F. Chang and J. G. McCarty, *Catal. Today*, 1996, **30**, 163-170.

29 (a) S. D. Aust, L. A. Morehouse and C. E. Thomas, *J. Free Radic. Biol. Med.*, 1985, **1**, 3-25; (b) B. A. Vanwinkle, K. L. D. Bentley, J. M. Malecki, K. K. Gunter, I. M. Evans, A. Elder, J. N. Finkelstein, G. Oberdorster and T. E. Gunter, *Nanotoxicology*, 2009, **3**, 307-318.

30 (a) B. Halliwell and J. M. C. Gutteridge, *Methods Enzymol.*, 1990, **186**, 1-85; (b) J. T. Hancock, R. Desikan and S. J. Neill, *Biochem. Soc. Trans.*, 2001, **29**, 345-350.

31 I. Gultekin, G. Tezcanli-Guyer and N. H. Ince, *Ultrason. Sonochem.*, 2009, **16**, 577-581.

32 R. Palominos, J. Freer, M. A. Mondaca and H. D. Mansilla, *J. Photoch. Photobio. A-Chem.*, 2008, **193**, 139-145.
33 P. D. Josephy, T. Eling and R. P. Mason, *J. Biol. Chem.*, 1982, **257**, 3669-3675.
34 W. Qin, L. Su, C. Yang, Y. Ma, H. Zhang and X. Chen, *J. Agric. Food Chem.*, 2014, **62**, 5827-5834.
35 W. Brandwilliams, M. E. Cuvelier and C. Berset, *LWT-Food Sci. Technol.*, 1995, **28**, 25-30.
36 R. Re, N. Pellegrini, A. Proteggente, A. Pannala, M. Yang and C. Rice-Evans, *Free Radic. Biol. Med.*, 1999, **26**, 1231-1237.
37 R. Pulido, L. Bravo and F. Saura-Calixto, *J. Agric. Food Chem.*, 2000, **48**, 3396-3402.

# Figures and Tables

**Figure captions**

**Scheme 1** The possible reaction mechanism of the TMB-$Mn_3O_4$ NPs system.

**Fig. 1** (A) SEM image and (B) XRD pattern of the as-obtained $Mn_3O_4$ NPs.

**Fig. 2** (A) The UV-vis absorbance spectrum of TMB in the absence of $H_2O_2$ and images of oxidation color reaction of TMB, ABTS and OPD by dissolved oxygen after catalyzing by $Mn_3O_4$ NPs. (B) The time-dependent absorbance changes at 655 nm of TMB with 5 mg/L $Mn_3O_4$ NPs in the absence of $H_2O_2$ and the effect of nitrogen on TMB oxidation. Conditions: $10^{-4}$ M TMB, 5 mg/L $Mn_3O_4$ NPs, 35 °C, pH 3.5 (0.2 M acetate buffer).

**Fig. 3** Steady-state kinetic assay of $Mn_3O_4$ NPs with TMB oxidation. The velocity ($v$) of the reaction was measured using 5 mg/L $Mn_3O_4$ NPs in pH 3.5 acetate buffer at 35 °C.

**Fig. 4** Effect of phenols on the TMB-$Mn_3O_4$ system and their relative activity in the F-C method.

**Fig. 5** UV-vis absorption spectra of TMB-$Mn_3O_4$ NPs system in the present of different concentrations of tannic acid. Inset: Standard calibration curve for tannic acid assay and the relative photographic images.

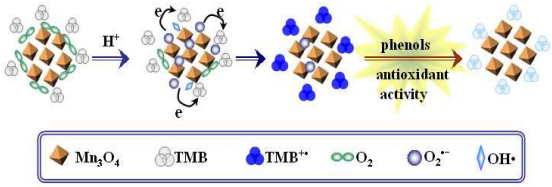


**Scheme 1**

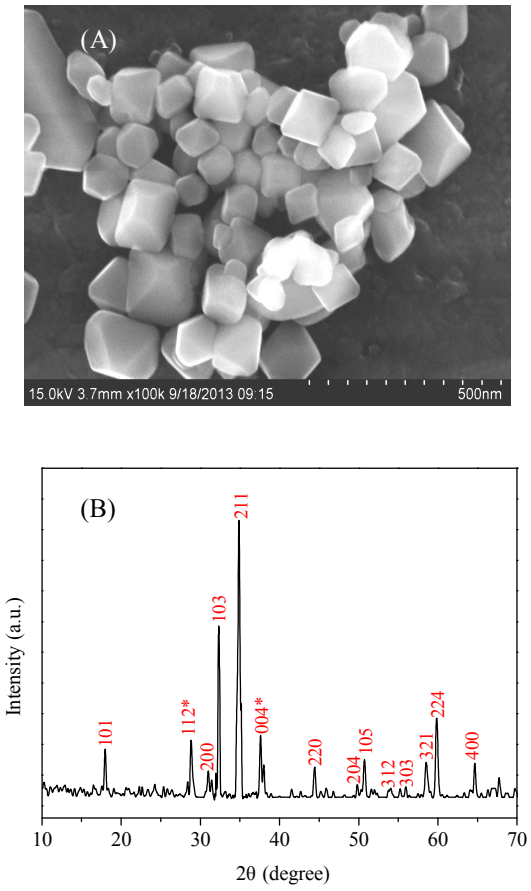


**Fig. 1**

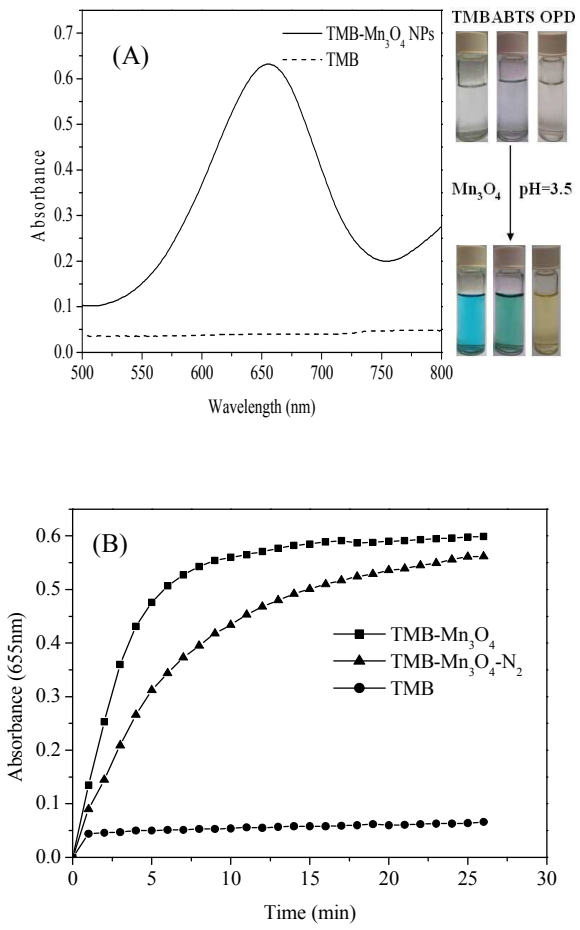


**Fig. 2**

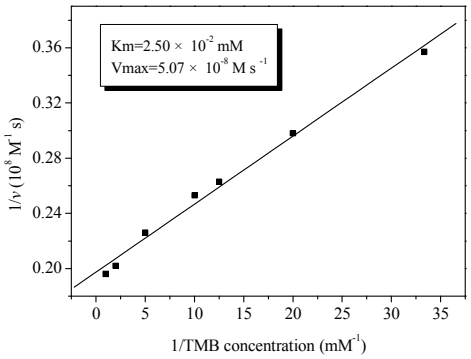


**Fig. 3**

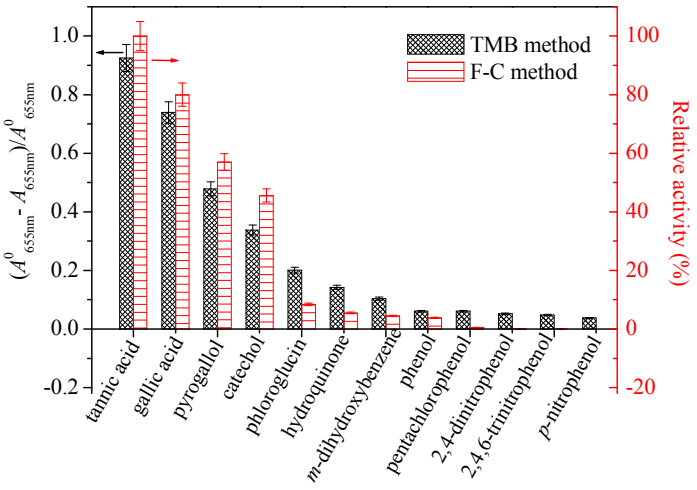


**Fig. 4**

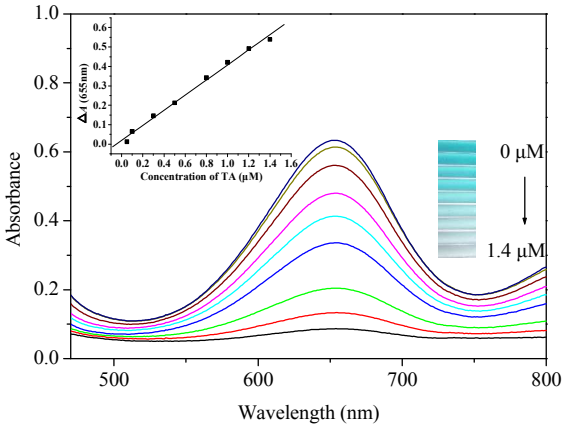


**Fig. 5**

**Table 1** Comparison of the kinetic parameters of oxidase mimetics

| Catalyst | $K_m$ [mM] | $V_{max}$ [$10^{-8}$ M $s^{-1}$] | Ref. |
|---|---|---|---|
| $Fe_3O_4$ NPs | 0.098 | 3.44 | 1 |
| Au@Pt nanorods | 0.006–0.013 | 2.5–2.62 | 6 |
| BSA-$MnO_2$ NPs | 0.039 | 5.8 | 7 |
| nanoceria | 0.8–3.8 | 30–70 | 14 |
| $Co_3O_4$ NPs | 0.051 | 3.30 | 34 |
| $Mn_3O_4$ NPs | 0.025 | 5.07 | This work |

# Graphical Abstract

$Mn_3O_4$ nano-octahedrons as effective oxidase mimic for the preliminary assessment of phenols' antioxidant activity and visual determination of tannic acid were demonstrated.